Printed ISSN 1330–0016
Online ISSN 1333–9133
CD ISSN 1333–8390
CODEN FIZBE7

SPIN-FLIP DOUBLETS OF ^{9}Be SPECTRUM WITHIN A CLUSTER MODEL

I. FILIKHIN, V. M. SUSLOV and B. VLAHOVIĆ

Department of Physics, North Carolina Central University, Durham, NC 27707, U. S. A.

Received 12 July 2011; Accepted 16 November 2011
Online 27 January 2012

The structure of the ^{9}Be low-lying spectrum is studied within the cluster model $\alpha+\alpha+n$. In the model, the total orbital momentum is fixed for each energy level. Thus each level is determined as a member of the spin-flip doublet corresponding to the total orbital momentum ($L^\pi = 0^+, 2^+, 4^+, 1^-, 2^-, 3^-, 4^-$) of the system. The Ali-Bodmer potential (model E) is applied for the $\alpha\alpha$ interaction. We employ a local αn potential which was constructed to reproduce the $\alpha - n$ scattering data. The Pauli blocking is simulated by the repulsive core of the s-wave components of these potentials. Configuration-space Faddeev equations are used to calculate the energy of the bound state ($E_{\rm calc} = -1.493$ MeV vs. $E_{\rm exp} = -1.5735$ MeV) and resonances. A variant of the method of analytical continuation in the coupling constant is applied to calculate energies of the low-lying levels. Available ^{9}Be spectral data are satisfactorily reproduced by the proposed model.

PACS numbers: 21.45.-v, 21.60.Gx, 21.80.+a UDC 539.142, 539.144
Keywords: few-body systems, cluster models, hypernuclei

1. *Introduction*

The ^{9}Be nucleus can be modeled as a typical cluster nuclear system with the neutron-halo structure. The three cluster model $\alpha+\alpha+n$ allows us to describe the ^{9}Be low-lying spectrum qualitatively [1]. In the last years, the cluster calculations for the ^{9}Be spectrum have been performed using different techniques and with different inter-cluster potentials [2−5]. The main problem of the cluster models is the adequate description of inter-cluster interactions. In particular, for an $\alpha+\alpha+n$ system, it is important to take into account the Pauli blocking for both the $\alpha\alpha$ and αn interactions. There exist two different methods of approximation for considering this problem. The first uses the process of elimination on the Pauli forbidden states caused by the potentials used. This procedure realizes the nonlocal potentials [5, 6]. The second uses the potentials which have a repulsive core to simulate the Pauli blocking [7, 8]. In this work we apply the second method of approximation. The inter-cluster potentials can be phenomenologically constructed by experimental data for the $\alpha\alpha$ and αn scattering. We used the known Ali-Bodmer potential (model E) [10] for the $\alpha\alpha$ interaction. The αn potential was constructed to reproduce the results of R-matrix analysis for the αn data [11]. In this way we adjusted the parameters of the αn potential taken from Refs. [8, 9]. Our goal is to obtain a new theoretical description for the ^{9}Be spectrum. Note that reliable ^{9}Be experimental data is restricted by the first several levels. In our model, the total orbital momentum is fixed for each level and, taking into account the spin of the neutron, each of the levels are determined as members of the spin-flip doublet corresponding to the total orbital momentum of the system. We consider the states of the $\alpha + \alpha + n$ system with $L^\pi = 0^+, 2^+, 4^+, 1^-, 2^-, 3^-, 4^-$. To calculate the energies of the low-lying levels, we applied the configuration-space Faddeev equations [12]. According to the proposed model, the partial decomposition of the Faddeev components of the total wave function was performed in the LS coupling scheme.

We found that the ^{9}Be spectral data are well reproduced within the proposed model. Thus we present a new classification of the ^{9}Be low-lying spectrum as a set of spin-flip doublets. A comparison of our results with the results obtained by different theoretical approaches supports our approximation as well. Predictions for the ^{9}Be spectrum are also presented.

2. *Formalism*

The Faddeev equations in coordinate space [12] are used for description of the ^{9}Be nucleus, considered as a three-body $\alpha\alpha n$ system. The general form of the equations is as follows:

$$\{H_0+V_\gamma^s(|\boldsymbol{x}_\gamma|)+\sum_{\beta=1}^{3} V_\beta^{\mathrm{Coul}}(|\boldsymbol{x}_\beta|)-E\}\Psi_\gamma(\boldsymbol{x}_\gamma,\boldsymbol{y}_\gamma) = -V_\gamma^s(|\boldsymbol{x}_\gamma|)\sum_{\beta\neq\gamma}\Psi_\beta(\boldsymbol{x}_\beta,\boldsymbol{y}_\beta), \quad (1)$$

where V_β^{Coul} is the Coulomb potential between the particles belonging to the pair β and V_γ^s is the short-range pair potential in the channel γ, (γ=1,2,3). $H_0 = -\Delta_{\boldsymbol{x}_\gamma} - \Delta_{\boldsymbol{y}_\gamma}$ is the kinetic energy operator, E is the total energy, and Ψ is the wave function of the three-body system. Ψ is given as a sum over three Faddeev components, $\Psi = \sum_{\gamma=1}^{3}\Psi_\gamma$. For the $\alpha\alpha\Lambda$ system including two identical particles, the coupled set of the Faddeev equations is written as

$$\begin{aligned}(H_0 + V_{\alpha n} + V^{\mathrm{Coul}} - E)W &= -V_{\alpha n}(U + P_{12}W),\\ (H_0 + V_{\alpha\alpha} + V^{\mathrm{Coul}} - E)U &= -V_{\alpha\alpha}(W + P_{12}W),\end{aligned} \quad (2)$$

where U is the Faddeev component corresponding to the rearrangement channel $(\alpha\alpha) - n$ and W corresponds to the rearrangement channel $(\alpha n) - \alpha$. The total wave function is expressed by the components U and W with the relation $\Psi = U + (1+P_{12})W$. P_{12} is the permutation operator for the α particles (particles 1,2), and $V_{\alpha\alpha}$ and $V_{\alpha n}$ are nuclear potentials of the $\alpha\alpha$ and αn interactions, respectively. $V^{\rm Coul}$ is the potential of Coulomb interaction between the α particles, The total orbital angular momentum is given by $\boldsymbol{L} = \boldsymbol{\ell}_{\alpha\alpha} + \boldsymbol{\lambda}_{(\alpha\alpha)-n} = \boldsymbol{\ell}_{\alpha n} + \boldsymbol{\lambda}_{(\alpha n)-\alpha}$, where $\ell_{\alpha\alpha}$ ($\ell_{\alpha n}$) is the orbital angular momentum of $\alpha\alpha$ (pair of αn) and $\lambda_{(\alpha\alpha)-n}$ ($\lambda_{(\alpha n)-\alpha}$) is the orbital angular momentum of a neutron (α particle) relative to the center of mass of the $\alpha\alpha$ pair and αn pair, respectively.

Possible combinations of relative momenta $\ell_{\alpha\alpha}$, $\lambda_{(\alpha\alpha)-n}$ and $\ell_{\alpha n}$, $\lambda_{(\alpha n)-\alpha}$ for the system with total orbital momentum L and parity π written as a block matrix are:

$$M(L^\pi) = \begin{pmatrix} (& \{\ell_{\alpha n}\} &) & (& \{\ell_{\alpha\alpha}\} &) \\ (& \{\lambda_{(\alpha n)-\alpha}\} &) & (& \{\lambda_{(\alpha\alpha)-n}\} &), \end{pmatrix}$$

where each block represents all quantum numbers taken into account. For example, the combinations corresponding to the 0^+ state can be given in the form

$$M(0^+) = \begin{pmatrix} (& 0 & 1 & 2 & \dots &) & (& 0 & 2 & 4 & \dots &) \\ (& 0 & 1 & 2 & \dots &) & (& 0 & 2 & 4 & \dots &). \end{pmatrix}$$

A more detailed description of this formalism is given in Ref. [13], applied to the cluster system $\alpha\alpha\Lambda$. For the system $\alpha\alpha n$, the spin-orbit coupling between the α-particle and the neutron is not negligible and we implement the spin-orbit part of the αn interaction into the formalism. The αn potential is written as a sum of the central and the spin-orbit parts: $V_{\alpha n} = V^{\rm c}_{\alpha n} + V^{\rm so}_{\alpha n}$. For the $\alpha\alpha n$ system in the LS basis the matrix elements of the spin-orbital potential $V^{\rm so}_{\alpha n}$ are given by the following form:

$$V^{\rm so}_{\alpha n}(r) = \frac{2L+1}{2} \sum_{j=l\pm 1/2} (2j+1) \begin{Bmatrix} J & L & 1/2 \\ l & j & \lambda \end{Bmatrix}^2 \tag{3}$$

$$\times (j(j+1) - l(l+1) - 3/4) v_{\rm so}(r),$$

where J is the total three-body angular momentum, L is the total three-body orbital momentum, j and l are total orbital momenta of the αn pair (the spin of the pair is equal to $\frac{1}{2}$), λ is the orbital momentum of the α-particle with respect to the center of the αn pair, and $v_{\rm so}(r)$ is a coordinate part of the αn spin-orbit potential.

The configurations of the angular momenta corresponding to the L^π states taken into account are represented below:

2^+ state

$$M(2^+) = \begin{pmatrix} (& 0 & 1 & 1 & 2 & 2 & 2 &) & (& 0 & 2 & 2 & 2 & 4 & 4 &) \\ (& 2 & 1 & 3 & 0 & 2 & 4 &) & (& 2 & 0 & 2 & 4 & 2 & 4 &) \end{pmatrix},$$

4^+ **state**

$$M(4^+) = \left(\begin{array}{c} (\ 0\ 1\ 2\ 2\ 3\ 4\ ) \\ (\ 4\ 3\ 2\ 4\ 1\ 0\ ) \end{array} \begin{array}{c} (\ 0\ 2\ 4\ 2\ 4\ 4\ ) \\ (\ 4\ 2\ 2\ 4\ 0\ 4\ ) \end{array} \right),$$

2^- **state**

$$M(2^-) = \left(\begin{array}{c} (\ 1\ 2\ 2\ 3\ 3\ 4\ ) \\ (\ 2\ 1\ 3\ 2\ 4\ 3\ ) \end{array} \begin{array}{c} (\ 2\ 2\ 4\ 4\ ) \\ (\ 1\ 3\ 1\ 3\ ) \end{array} \right),$$

4^- **state**

$$M(4^-) = \left(\begin{array}{c} (\ 1\ 2\ 2\ 3\ 4\ 4\ ) \\ (\ 4\ 3\ 5\ 2\ 1\ 3\ ) \end{array} \begin{array}{c} (\ 2\ 2\ 4\ 4\ ) \\ (\ 3\ 5\ 1\ 3\ ) \end{array} \right),$$

3^- **state**

$$M(3^-) = \left(\begin{array}{c} (\ 0\ 3\ 2\ 1\ 1\ 4\ ) \\ (\ 3\ 0\ 1\ 2\ 4\ 1\ ) \end{array} \begin{array}{c} (\ 0\ 2\ 2\ 4\ 4\ ) \\ (\ 3\ 1\ 3\ 1\ 3\ ) \end{array} \right),$$

1^- **state**

$$M(1^-) = \left(\begin{array}{c} (\ 0\ 1\ 1\ 2\ 2\ 3\ ) \\ (\ 1\ 0\ 2\ 1\ 3\ 2\ ) \end{array} \begin{array}{c} (\ 0\ 2\ 2\ 4\ 4\ ) \\ (\ 1\ 1\ 3\ 3\ 5\ ) \end{array} \right).$$

3. Potentials

Nuclear $\alpha\alpha$ interaction is given by the phenomenological Ali-Bodmer (AB) potential [10]. This potential has the following form: $V_{\alpha\alpha}(r) = \sum_{l=0,2,4} V^l_{\alpha\alpha}(r) P_l$, where P_l is a projector onto the state of the $\alpha\alpha$ pair with the orbital momentum l. The functions $V^l_{\alpha\alpha}(r)$ have the form of one or two range Gaussians:

$$V^l_{\alpha\alpha}(r) = V^l_{\rm rep} \exp(-\beta^l_{\rm rep} r)^2 - V^l_{\rm att} \exp(-\beta^l_{\rm att} r)^2 \ . \tag{4}$$

The s-wave component $V^0_{\alpha\alpha}(r)$ has a strong repulsive core which simulates Pauli blocking for the α's at short distances. There are different sets of the parameters for partial components $V^l_{\alpha\alpha}(r)$ [10]. The parameters of the version "e" of the Ali-Bodmer potential (ABe) are given in Table 1.

The αn interaction in s, p and d states is taken into account (Fig. 1). The p and d-wave components include central and spin-orbit parts:

$$V^{jl}_{\alpha n}(r) = v^l_{\rm c}(r) + (\boldsymbol{s}, \boldsymbol{l}) v_{\rm so}(r), \tag{5}$$

where $\boldsymbol{j} = \boldsymbol{l} + \boldsymbol{s}$, $\boldsymbol{s}$ is the spin of the neutron. The coordinate dependencies of the components have the form of one- or two-range Gaussians. The s-wave component

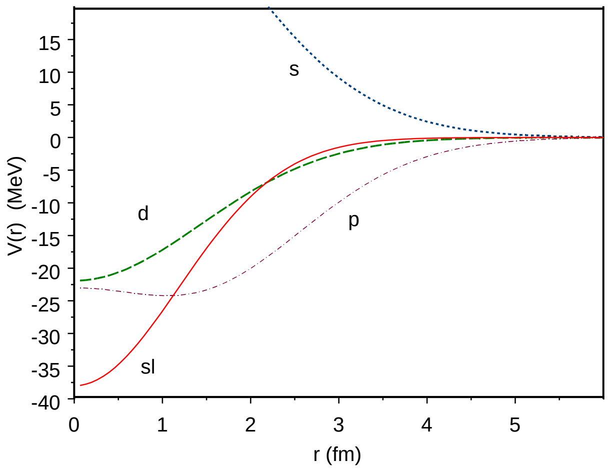

Fig. 1. Partial (s, p, d) and spin-orbit (sl) components of the $\alpha - n$ potential.

TABLE. 1. Parameters of the $\alpha\alpha$ (ABe [10]) and αn potentials. The pair-orbital momentum is l. $V^l_{\rm att}$, ($V^l_{\rm rep}$) and V_c are given in MeV, *$\beta^l_{\rm att}$ ($\beta^l_{\rm rep}$) in* fm^{-1} *and α_c in* fm^{-2}.

Interaction	Potential	l	$V^l_{\rm rep}$	$\beta^l_{\rm rep}$	$V^l_{\rm att}$	$\beta^l_{\rm att}$
$\alpha\alpha$	central	0	1050	0.8	150	0.5
		2	640	0.8	150	0.5
		4	–	–	150	0.5
αn	central	0 [8]	50.0	1/2.3	–	–
		1	40.0	1/1.67	63.0	1/2.3
		2 [9]	–	–	21.93	1/2.03
	spin-orbit	–	–	–	38.0	1/1.67

has a repulsive core [7−9] to simulate the s state Pauli exception for $\alpha - n$. The d-wave component of the αn potential was taken from Ref. [9]. In this work we propose a modification for the p-wave and spin-orbit components of the potential given in [9]. The parameters of our potential are listed in Table 1. The goal of the modification is to reach a better description for the $\alpha - n$ scattering data. For experimental data, we used the results of the R-matrix analysis of the data from [11]. In Fig. 2, the phase shifts for the $\alpha - n$ scattering are given to compare our results with the proposed potential and the R-matrix fit. We have obtained strong agreement between the two results for neutron energies up to $4-5$ MeV.

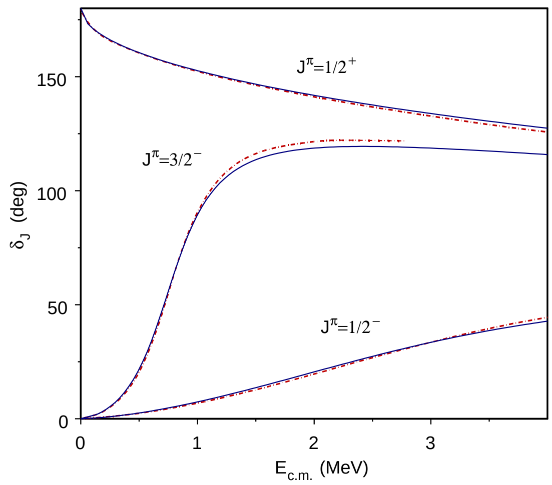

Fig. 2. Phase shifts for $\alpha - n$ scattering. Solid curves are our results with potential (5) and dot-dashed curves are an R-matrix fit to data from [11].

4. Methods

The bound state problem based on the configuration-space Faddeev equations (1) for the $\alpha\alpha n$ system (Eq. (2)) is solved numerically by applying the finite-difference approximation with spline collocation method [13, 15]. For calculation of the eigenvalues, the method of inverse iterations is used. To estimate the energies and widths of the low-lying resonance states, we applied the method of analytical continuation in the coupling constant [16]. A variant of this method with an additional non-physical three-body potential is used. The strength parameter of this potential is considered as a variational parameter for the analytical continuation of the bound state energy into the complex plane [17−19]. This potential, considered as a perturbation to the corresponding three-body hamiltonian, is added to the left-hand-side of Eqs. (2). The three-body potential has the form:

$$V_3(\rho) = -\delta \exp(-b\rho^2), \tag{6}$$

where b is a range parameter of this potential ($b = 0.008$ fm^{-2}) and δ is a strength parameter (variational parameter), $\delta \geq 0$. $\rho^2 = x_\alpha^2 + y_\alpha^2$, where x_α, y_α are the mass scaled Jacobi coordinates ($\alpha = 1, 2$) [14]. For each resonance, there exists a region $|\delta| \geq |\delta_0|$ where a resonance becomes a bound state. In this region we obtain the $2N$ three-body bound state energies corresponding to $2N$ values of δ. 2N is the number of points used in the real energy plane for construction of the Padé approximation. The continuation of the energy into the complex plane is carried out by means of the Padé approximation: $\sqrt{-E} = \sum_{i=1}^{N} p_i\xi^i \Big/ \Big[1 + \sum_{i=1}^{N} q_i\xi^i\Big]$, where $\xi = \sqrt{\delta_0 - \delta}$

and p_i and q_i are calculated parameters. The Padé approximation for $\delta = 0$ gives the energy and width of the resonance: $E(\delta = 0) = E_r + \mathrm{i}\Gamma/2$. The accuracy of the Padé approximation for resonance energy and width depends on a few parameters, the distance from the scattering threshold, the accuracy of calculation for bound states and determination of δ_0. Calculated resonance energy can depend on the order N of the Padé aproximants used (for example, see Ref. [20]).

5. *Calculations*

The bound state of the $\alpha\alpha n$ system, having negative ("natural" [5])) parity with $J^\pi = (\frac{3}{2})^-$ and $L^\pi = 1^-$, is associated with the ground state of the $^9_\Lambda$Be hypernucleus. The experimental value for this state is 1.5735 MeV [22]. This state is lower member of the spin-flip doublet with orbital momentum $L = 1$. The upper member of this doublet is the resonance state $J^\pi = (\frac{1}{2})^-$ with energy 1.21 ± 0.12 MeV. Calculated values (~ 0.9 MeV) for this doublet are close to the experimental data. The calculated spin-doublet spacing is about 2.4 MeV, whereas the experimental value is about 2.68 ± 0.12 MeV. In Table 2, we give the ^{9}Be ground state binding energy calculated for various orbital momentum configurations. Orbital momentum configurations $l^\pi = 0^+$ and 2^+ of the core nucleus ^{8}Be contribute significantly to the ^{9}Be ground state energy. A weakly bound state of the $\alpha\alpha n$ system is possible if the $l^\pi = 0^+$ configuration is taken into account. Addition of the $l^\pi = 2^+$ configuration of the $\alpha\alpha$ pair gives the final value for the binding energy. Meanwhile, the contribution of the configuration $l^\pi = 4^+$ is relatively small.

TABLE. 2. Binding energy E_B of the ^{9}Be ground state ($3/2^-$) (in MeV), calculated for various orbital momentum configurations. Energy is measured with respect to the $\alpha + \alpha + n$ threshold. Experimental value is E_B^{ex}=-1.5735 MeV [22].

$\{(l_{\alpha n},\lambda_{(\alpha n)-\alpha})\}$	$\{(l_{\alpha\alpha},\lambda_{(\alpha\alpha)-n})\}$	E_B
(0,1)	(0,1)	unbound
(0,1)(1,0)(1,2)(2,1)		unbound
(0,1)(1,0)(1,2)(2,1)(2,3)		-0.032
(0,1)(1,0)(1,2)(2,1)(2,3)(3,2)		-0.042
(0,1)	(2,1)	unbound
(0,1)(1,0)(1,2)(2,1)(2,3)(3,2)		unbound
	(0,1)(2,1)	-1.403
	(0,1)(2,1)(2,3)	-1.480
	(0,1)(2,1)(2,3)(4,3)	-1.492
	(0,1)(2,1)(2,3)(4,3)(4,5)	-1.493

Results of our calculation for the low-lying spectrum of ^{9}Be are given in the third column of Table 3. The next two columns include the results of Refs. [2, 3, 24]. Experimental data for ^{9}Be ($T = 1/2$) is given in the last column of this table. Each energy level is classified as a member of the spin-flip doublet corresponding to the total orbital momentum $L^\pi = 0^+, 2^+, 4^+, 1^-, 2^-, 3^-, 4^-$ of the $\alpha\alpha n$ system. Our model's predicted results correlate well with the experimental data [23]. In our opinion, the neutron-halo structure of the ^{9}Be is the reason for the possibility of classification.

To give an overall evaluation of our results, we present a relation between the calculated and experimental spectrum of ^{9}Be in Fig. 3. In this figure, the solid

TABLE. 3. Energy levels in the $\alpha\alpha n$ system and low-lying ^{9}Be spectrum. Results of our calculations are presented in the third column. The energy (in MeV) is measured from the $\alpha + \alpha + n$ threshold. Experimental data for ^{9}Be ($T = 1/2$) are taken from [23].

L^π	J^π		[2] (CSM)	[3]	[24]*	Exp.
0^+	$\frac{1}{2}^+$	0.3(4)	–	–	–	0.111±0.007
1^-	$\frac{3}{2}^-$	-1.493	-2.16	-1.60	-1.48(4)	-1.5735
	$\frac{1}{2}^-$	0.9(0)	1.06	–	2.24(6)	1.21±0.12
2^-	$\frac{5}{2}^-$	0.7(2)	0.39	–	0.73(6)	0.8559±0.0013
	$\frac{3}{2}^-$	2.(7)	2.88	2.65	–	4.02±0.1 or 3.4±0.5[25]
2^+	$\frac{5}{2}^+$	1.(8)	1.75	–	–	1.476±0.009
	$\frac{3}{2}^+$	3.(0)	3.21	–	–	3.1312±0.025
3^-	$\frac{7}{2}^-$	4.(6)	5.02	–	5.03(6)	4.81±0.06
	$\frac{5}{2}^-$	6.(4)	6.57	–	–	6.36±0.08
4^+	$\frac{9}{2}^+$	5.(1)	5.04	–	–	5.19±0.06
	$\frac{7}{2}^+$	6.(6)	6.80	–	–	–
4^-	$\frac{9}{2}^-$	8.(6)	9.73	–	8.62(6)	–
	$\frac{7}{2}^-$	10.(7)	–	–	–	–

*Quantum Monte Carlo calculations for $A = 9$.

line indicates the root-mean-square fit for this correlation. The fitted line is close to the line (dashed line in Fig. 3) showing the ideal situation when calculated values coincide with experimental data. These two lines are practically identical. The slight angle difference between the lines is due to a relatively large disagreement between the calculated and experimental values for the $J^\pi = 3/2^-$ ($L^\pi = 2^-$) and $J^\pi = 5/2^+$ ($L^\pi = 2^+$) states. Note that other cluster calculations [2, 3] (see Table 3) demonstrate the same disagreement with the experimental data. We note that there is experimental evidence [25] for the wide $J^\pi = (\frac{3}{2})^-$ resonance with energy of 3.4±0.5 MeV that is closer to the calculated values.

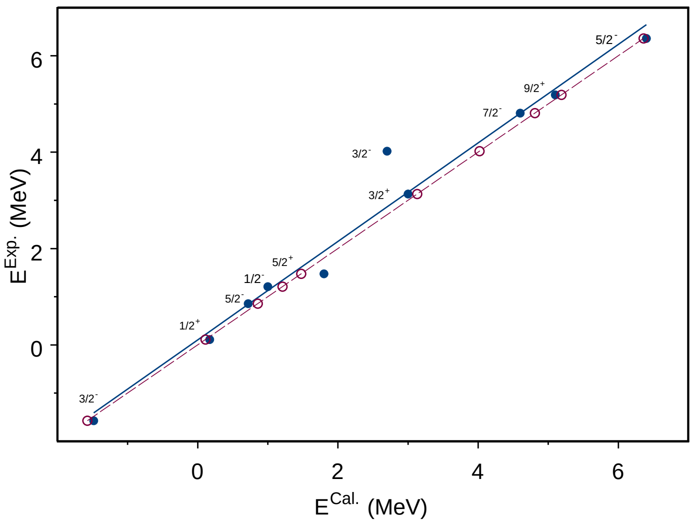

Fig. 3. Correlation between calculated (Cal.) and experimental (Exp.) spectrum of ^{9}Be *(solid dots). Solid line is the root mean square fit for the correlation. The dashed line shows the ideal situation when the calculated values coincide with experimental data (open dots). Total momentum of each level is shown.*

Our calculations strongly agree with the previous ^{9}B calculations [2, 24]. In particular, we confirm that the $J^\pi = 7/2^+$ and $J^\pi = 9/2^-$ resonances have the excited energies about 10 MeV and 8 MeV, respectively. Energy of the resonance $J^\pi = 7/2^-$, as an upper member of the level $L^\pi = 4^-$, was predicted with approximately an excitation energy of 12 MeV.

The mirror nucleus ^{9}B can also be considered using the present cluster model after the replacement of neutron by proton. Obviously, this replacement must include the changes in mass and potential. To evaluate the effect of the potential replacement, we calculated the first energy levels of the $\alpha\alpha p$ system with the α-n potential which was used for the $\alpha\alpha n$ calculations. Results of our calculations for several levels are given in Table 4. We compare these results with experimental data for ^{9}Be and ^{9}B. The Coulomb energy Δ_c is calculated as the energy difference between corresponding levels of ^{9}Be and ^{9}B, measured from the $\alpha + \alpha + n$ and $\alpha + \alpha + p$ thresholds, respectively. This energy includes the result of the change in mass which has to be excluded from this difference. Note that the mass difference of proton and neutron is about 1.293 MeV. From Table 4, it is clear that the α-n potential used instead of the appropriate α-n potential in the $\alpha\alpha p$ system leads to systematical overbinding (about 0.25 MeV and more) for the $\alpha\alpha p$ system relative to the experimental data. The Coulomb energy Δ_c is slightly less (about 0.15 MeV) than the experimental value which is in conflict with this overbinding. One can conclude that the α-p potential has to differ from the α-n potential in both the strength and range parameters. Nevertheless, the obtained results qualitatively keep the structure of the ^{9}B low-lying spectrum given by the experimental data.

TABLE. 4. Results of our calculations for several energy levels in the $\alpha\alpha p$ system and low-lying ^{9}B spectrum. The energy E (in MeV) is measured from the $\alpha+\alpha+p$ threshold. The Coulomb energy Δ_c of proton displacement in $\alpha\alpha n$ system (in MeV) of each level is presented. Experimental data (denoted as "Exp.") for ^{9}B ($T=1/2$) are taken from Ref. [23].

L^π	J^π	E	Δ_c	$E^{\mathrm{Exp.}}$	$\Delta_c^{\mathrm{Exp.}}$
1^-	$\frac{3}{2}^-$	0.1(6)	0.4	0.277	0.56
	$\frac{1}{2}^-$	2.(4)	0.1	3.027±0.3	0.25
2^-	$\frac{5}{2}^-$	2.(4)	0.4	2.6386±0.005	0.49

Finally, our calculations for resonances are illustrated in Figs. 4 and 5. In the first one, the real parts of the Páde approximants for the $(\frac{3}{2}^-, \frac{5}{2}^-)$ spin flip doublet of ^{9}Be are shown. The total orbital momentum and parity of each level are 2^-. Calculations for several values of the strength parameter δ (see Eq. (6)) give a "trajectory" of negative energies (noted by circles in Fig. 4). Real parts of the constructed Páde approximants are shown by lines. Resonance energies of both levels correspond to the zero value of the argument δ (δ =0). From Fig. 4, one can see that the behavior of the Páde approximants is close to linear dependence. The

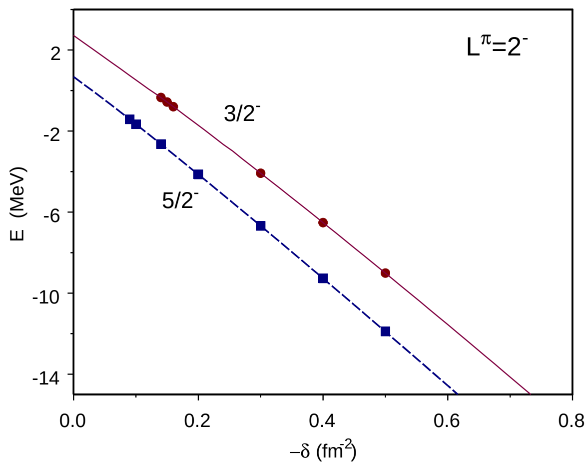

Fig. 4. The Páde approximants for the spin-flip doublet $(\frac{3}{2}^-, \frac{5}{2}^-)$ of ^{9}Be. Total orbital momentum and parity of each level are 2^-. Bound state energies calculated for several values of δ (see Eq.(6)) are depicted by the circles and squares for the $\frac{3}{2}^-$ and $\frac{5}{2}^-$, respectively. Real parts of the Páde approximants are shown by lines. Resonance energy is found at δ=0 (Here we used the value $\hbar^2/2m$=41.44 MeV fm^2 for conversion of MeV to fm^{-2}). Energy is measured from $\alpha+\alpha+n$ threshold.

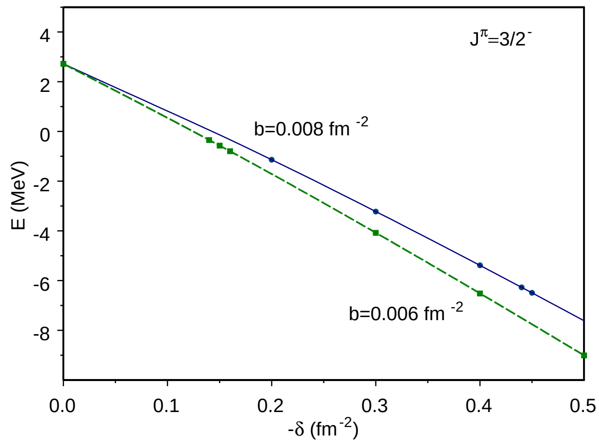

Fig. 5. The Páde approximants for the the upper member $\frac{3}{2}^-$ of the $L = 2^-$ state of ^{9}Be. The calculation of resonance energy was performed for two values of the range parameter b of the tree-body potential (6). All notations are the same as in Fig. 4.

energies may be determined just as well by eye as by calculation due to the linear behavior of the Páde approximants. In Fig. 5, the Páde approximants for the $\frac{3}{2}^-$ upper member of the $L = 2^-$ state is shown for two values of the range parameter b of the three-body potential (6). The real parts of the obtained Páde approximants are crossed at point $\delta = 0$. It is a test for our calculations. We have obtained from Fig. 5 that the non-physical three-body potential with different values for the parameter b gives different Páde approximants. However, the calculated resonance energy does not depend on this parameter. We can conclude that the value obtained for resonance energy corresponds to the physical value. Non-physical solutions, which are possible using this method, can be separated by this test.

6. Summary

The configuration-space Faddeev equations were applied to calculate the energy spectrum of the ^{9}Be nucleus within the $\alpha + \alpha + n$ cluster model. We found the set of local phenomenological potentials which accurately reproduce the ground state binding energy and reasonably reproduce the energies of low-lying resonances. This set includes the Ali-Bodmer potential of the model "e" for $\alpha\alpha$ and a new αn potential, which was constructed to reproduce the R-matrix fit for the αn scattering data. In our model the total orbital momentum is fixed for each energy level. Thus, the ^{9}Be energy levels can be classified as members of the spin-flip doublet corresponding to the total orbital momentum ($L^\pi = 0^+, 2^+, 4^+, 1^-, 2^-, 3^-, 4^-$) of the system. In the framework of the model, the predictions for the resonance energies of the 4^+ and 4^- spin flip-doublets have been made. For the ^{9}B nucleus, considered within cluster model $\alpha+\alpha+p$, we found that the αp potentials have to differ from the αn potential in both strength and range parameters.

Acknowledgements

This work was supported by NSF CREST award HRD-0833184 and NASA award NNX09AV07A. The numerical calculations were performed by High Performance Computing Center of the North Carolina State University.

References

[1] Y. C. Tang, F. C. Khanna, R. C. Herndon and K. Wildermuth, Nucl. Phys. **35** (1962) 421.

[2] K. Arai, P. Descouvemont, D. Baye and W. N. Catford, Phys. Rev. C **68** (2003) 014310.

[3] R. Álvarez-Rodríguez, A. S. Jensen, E. Garrido and D. V. Fedorov, Phys. Rev. C **82** (2010) 034001.

[4] M. Theeten D. Baye and P. Descouvemont, Phys. Rev. C **74** (2006) 044304.

[5] M. Theeten, H. Matsumura, M. Orabi, D. Baye, P. Descouvemont, Y. Fujiwara and Y. Suzuki Phys. Rev. C **76** (2007) 054003.

[6] E. Hiyama, M. Kamimura, T. Motoba, T. Yamada and Y. Yamamoto, Phys. Rev. C **66** (2002) 024007.

[7] S. Sack, L. C. Biedenharn and G. Bret, Phys. Rev. **93** (1954) 321.

[8] M. V. Zhukov, B. V. Danilin, D. V. Fedorov, J. M. Bang, I. J.Thompson and J. S. Vaagen, Phys. Rep. **231** (1993) 151.

[9] D. V. Fedorov, A. S. Jensen and K. Riisager, Phys. Rev. C **49** (1994) 201; A. Cobis, D. V. Fedorov and A. S. Jensen, Nucl. Phys. A **631** (1998) 793.

[10] S. Ali and A. R. Bodmer, Nucl. Phys. **80** (1966) 99.

[11] K. M. Nollett, S. C. Pieper, R. B. Wiringa, J. Carlson and G. M. Hale, Phys. Rev. Lett. **99** (2007) 022502.

[12] L. D. Faddeev and S. P. Merkuriev, *Quantum Scattering Theory for Several Particle Systems* Kluwer Academic, Dordrecht (1993) pp. 398.

[13] I. Filikhin, A. Gal and V. M. Suslov, Nucl. Phys. A **743** (2004) 194.

[14] I. Filikhin, V. M. Suslov and B. Vlahović, J. Phys. G: **30** (2004) 513.

[15] J. Bernabeu, V. M. Suslov, T. A. Strizh and S. I. Vinitsky, Hyperfine Interaction **101/102** (1996) 391.

[16] V. I. Kukulin, V. M. Krasnopolsky and J. Horacek, *Theory of Resonances*, Kluwer Academic, Dordrecht (1989).

[17] C. Kurokawa and K. Kato, Phys. Rev. C **71** (2005) 021301(R).

[18] I. Filikhin, V. M. Suslov and B. Vlahović, J. Phys. G **31** (2005) 1207.

[19] I. Filikhin, V. M. Suslov and B. Vlahović, Phys. Atom. Nucl. **72** (2009) 619.

[20] R. Lazauskas and J. Carbonell, Phys. Rev. C **71** (2005) 044004.

[21] D. V. Fedorov, A. S. Jensen, Phys. Lett. B **389** (1996) 631.

[22] Nuclear data evaluation project, http://www.tunl.duke.edu/nucldata/.

[23] D. R. Tilley, J. H. Kelley, J. L. Godwin, D. J. Milliner, J. E. Purcell, C. G. Sheu, H. R. Weller, Nucl. Phys. A **745** (2004) 155; http://www.tunl.duke.edu/nucldata/.

[24] S. C. Pieper, K. Varga and R. B. Wiringa1, Phys. Rev. C **66** (2002) 044310.

[25] Y. Prezado et al., Phys. Lett. B **618** (2005) 43.

STANJA SPINSKIH DUBLETA U SPEKTRU ^{9}Be U MODELU GROZDOVA

Proučavaju se niskoležeća stanja ^{9}Be polazeći od modela grozda $\alpha+\alpha+n$. Za svako stanje se uzima određen ukupni moment impulsa. Tako je svako stanje određeno kao član spinskih dubletnih stanja s danim ukupnim momentom impulsa sustava ($L^\pi = 0^+, 2^+, 4^+, 1^-, 2^-, 3^-, 4^-$). Primjenjuje se Ali-Bodmerov potencijal (model E) za međudjelovanje $\alpha\alpha$. Za međudjelovanje αn primjenjuje se lokalni αn potencijal, koji se podešava kako bi se postigao sklad s podacima za $\alpha - n$ raspršenje. Paulijeva zabrana se postiže s odbojnom jezgrom za s valove tih potencijala. Za računanje energije vezanog stanja ($E_{\rm calc} = -1.493$ MeV vs. $E_{\rm exp} = -1.5735$ MeV) i rezonancija rabe se Faddeevljeve jednadžbe u običnom prostoru. Za računanje energija niskoležećih stanja primjenjuje se inačica metode za analitičko nastavljanje konstante međudjelovanja. Ovim modelom postižemo dobar sklad s poznatim spektralnim podacima za ^{9}Be.